C. T. Savell
Manager,
Theorectical Aeroacoustics,
General Electric Co.,
Evendale, Ohio

W. R. Wells
Assoc. Professor,
University of Cincinnati,
Cincinnati, Ohio,
Mem. ASME

Rotor Design to Attenuate Flow Distortion

Part I A Semiactuator Disk Analysis

The transfer of stationary circumferential inlet distortion through a rotor is analyzed using unsteady semiactuator disk cascade theory. This method models the blade cascade as one-dimensional wave guides and describes the transmission characteristics of a rotor to be a function of the distortion wave length and the length of the rotor chord, as well as the normal design parameters. Two parametric studies on the response of a loaded rotor to inlet distortions are done for a single rotor operating at off design conditions and a number of rotors operating at their design points. Fourier series representations of arbitrary distortion wave shapes are used for comparison with experimental data.

Introduction

Numerous experiments [1, 2, 3][1] have shown the transmission characteristics of a rotor to be a function of the distortion wavelength and the length of the rotor chord. The present work is the first analysis to systematically include these effects by using compressible semiactuator disk (SAD) theory. Semiactuator disk theory has been applied previously to the cascade problems of stall flutter by Tanida and Okazaki, [8] transmission of sound by Kaji and Okazaki [9] and general resonance criteria by Alford [10].

In the present formulation it is assumed that the flow field on either side of the rotor is inviscid and two dimensional. The radial effects which are experienced in an axial flow compressor are ignored so the analysis is more appropriate for a rotor with a high hub-to-tip ratio. The time steady flow parameters are assumed constant values on either side of the blade row with a jump discontinuity at the blade leading edge. The rotor blade cascade is modeled as a set of one-dimensional wave guides. The amplitude of the distortion is considered to be small relative to the mean flow levels.

The solution to the problem essentially rests on solving and coupling the three flow fields shown in Fig. 1. For the upstream field, an inlet distortion pattern, represented by a total pressure and flow defect with a uniform static pressure, is imposed on the mean flow ahead of the rotor. For a coordinate system fixed with the rotor this pattern appears as a shear wave harmonic in time with a period corresponding to the number of distortion zones per revolution.

The resulting linearized equations of motion can accommodate a second disturbance in the upstream field in addition to the imposed shear wave. In general, the second field can have static pressure variations in addition to changes in velocity and will decay in amplitude with distance from the rotor. The particle velocity disturbances which accompany the static pressure waves tend to wash out the incident axial velocity distortion and create swirl velocity distortion near the rotor to support the static pressure gradients.

Downstream of the cascade both a shear wave and pressure wave again exist with amplitudes depending upon the transmission characteristics of the rotor.

The semiactuator disk approximation occurs in evaluating the third field within the cascade. The assumption of infinitesimal blade spacing makes it possible to treat the flows and wave propagation within the cascade as one-dimensional. Disturbances are transmitted through the blading as plane waves with their fronts perpendicular to the airfoil surface. This wave description automatically satisfies the airfoil boundary condition that no flow can pass through the blade surface.

One can interpret a semiactuator disc cascade as a plane layer whose acoustic impedance is different from air so that the reflected wave and transmitted wave from the layer are produced at the leading edge and the trailing edge line of the cascade respectively. Communication between the leading and trailing edge lines is established by the plane waves traveling within the cascade.

Five unknown waves in addition to the imposed shear wave have been identified:

1 The upstream pressure wave;
2 the leading edge to trailing edge traveling plane wave within the cascade;
3 the trailing edge to leading edge traveling plane wave within the cascade;
4 the downstream pressure wave;
5 the downstream shear (or vorticity) wave.

To determine the amplitude of each wave, five boundary or coupling conditions must be used. Following Ehrich [7] and Kaji [9] these conditions are:

[1] Numbers in brackets designate References at end of paper.

Contributed by the Gas Turbine Division and presented at the Gas Turbine Conference, Zurich, Switzerland, March 31–April 4, 1974, of THE AMERICAN SOCIETY OF MECHANICAL ENGINEERS. Manuscript received at ASME Headquarters, November 27, 1973. Paper No. 74-GT-41.

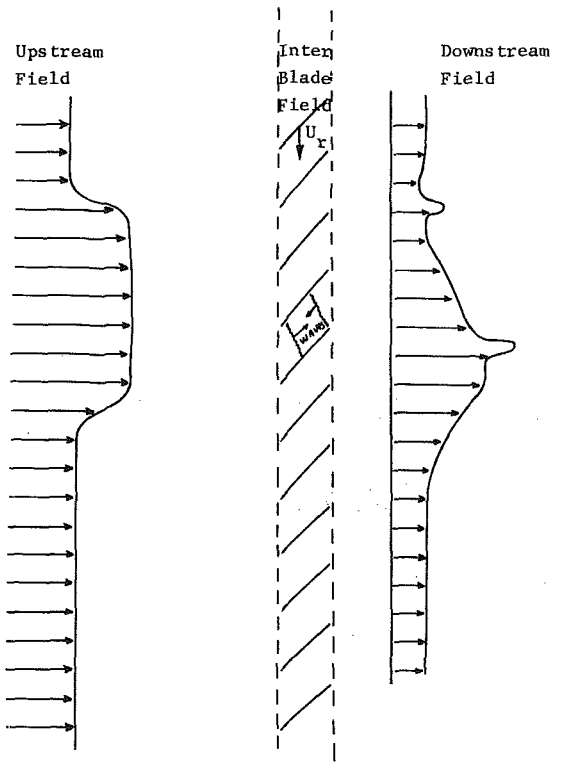

Fig. 1 Flow field representation

1 Mass flow is continuous at the leading edge line;
2 total enthalpy is conserved at the leading edge line;
3 mass flow is continuous at the trailing edge line;
4 total enthalpy is conserved at the trailing edge line;
5 the flow direction at the trailing edge is determined by the Kutta-Joukowski condition.

The key to amplification or attenuation of total pressure distortion is the Kutta-Joukowski condition. This assumption introduces a limiting effect of viscosity into our inviscid system of equations by requiring the flow to leave the airfoil trailing edges smoothly and parallel to the plates. The condition is necessary mathematically to insure a unique solution to the problem and has been verified by experiments.

As the flat plate rotor passes through the distorted flow changes in local incidence angle occur. The Kutta condition implies the flow leaves the rotor at a constant exit-angle. Hence, excursions in angular momentum occur within the rotor which create changes in the local total pressure distortion. In the semi-actuator disk theory a singularity occurs at the leading edge of the cascade, so that the flow turns suddenly at the leading edge line. Therefore, the momentum flux is discontinuous across the leading edge line even though the mass flux and energy flux is continuous by conditions 1 and 2.

The Governing Equations

The conservation equations for an ideal, inviscid, isentropic, compressible fluid with no body forces can be reduced to a linearized form if it is assumed that the (unsteady) perturbations around the (steady) time averaged quantities are of such small amplitude that only linear terms in the perturbation need be con-

Nomenclature

A_I, A_R = amplitude of the axial velocity distortion
AR = area ratio = $A1/A2$
a_1, a_4 = tangent of the absolute flow angle
$\bar{B}_j$ = column vector element
b = blade chord
b_2, b_3 = tangent of the relative flow angle
C_θ = tangential velocity in relative reference frame
C_Z = axial velocity
$\bar{C}_{ij}$ = coefficient matrix element
$\bar{c}$ = speed of sound
D_u, D_0 = amplitude of wave traveling within cascade
$d_1, d4$ = function defined by equation (15)
e_1, e_4 = function defined by equation (15)
f_1, f_4 = function defined by equation (15)
g = parameter defined by equation (A2)
h = (1) static enthalpy
= (2) parameter defined by equation $A2$
i = (1) $\sqrt{-1}$
= (2) tensor subscript
j = tensor subscript
k = reduced frequency = $\frac{\omega b}{U}$
M = relative Mach number
M_z = axial Mach number
m = (1) index
= (2) parameter defined by equation (A2)
n = (1) general index
= (2) parameter defined by equation (A2)
P = functional form of the static pressure in the axial direction
P_T = total pressure
p = static pressure
q = absolute velocity vector
q_x = velocity perturbation in axial direction
q_y = velocity perturbation in direction of rotor rotation
r_1, r_4 = function defined by equation (15)
SAD = semi-actuator disk method
s = spacing between adjacent blades with the cascade
T_T = total temperature
t = time
U = relative velocity
U_r = rotor speed
u' = velocity perturbation along the chord
X = functional form of the axial velocity perturbation in the axial direction
$\bar{X}_i$ = unknown column vector
Y = functional form of the tangential velocity perturbation in the axial direction
y = coordinate in the direction of rotor rotation in the relative reference frame
y_0 = phase shift
z = coordinate in axial direction
α_1, α_2 = absolute flow angle
β_1, β_2 = relative flow angle
γ = ratio of specific heats
$\Delta(\ )$ = distortion quantity which persists far from the blade row
ϵ = amplitude of axial velocity distortion
ϕ = phase shift of the axial velocity distortion
Ξ = functional form of the partial velocity fluctuation along the blade chord
θ = coordinate in direction of rotor rotation absolute reference frame = $y + U_r t$
π = 3.14159 . . .
ρ = static density
ω = circular frequency of disturbance
λ = distortion wavelength
ξ = coordinate along the blade chord
σ = cascade solidity = b/s

Subscripts

$(\ )_1$ = at far upstream infinity
$(\ )_2$ = disturbance ahead of the rotor due to the rotor
$(\ )_3$ = disturbance behind the rotor due to the rotor
$(\ )_4$ = at far downstream infinity
$(\ )_l$ = at leading edge
$(\ )_t$ = at trailing edge

sidered. The perturbation equations are:

Continuity:

$$\frac{\partial \rho'}{\partial t} + \nabla \cdot (\rho' \underline{\bar{q}} + \bar{\rho} \underline{q}') = 0 \tag{1}$$

Momentum:

$$\frac{\partial \underline{q}'}{\partial t} + (\underline{\bar{q}} \cdot \nabla)\underline{q}' + (\underline{q}' \cdot \nabla)\underline{\bar{q}} = -\frac{1}{\bar{\rho}} \nabla p' + p' \frac{\nabla \bar{p}}{\bar{\rho}^2} \tag{2}$$

Equation of State:

$$p' = \bar{c}^2 \rho' \tag{3}$$

Assuming the mean quantities are constant in space and time one can combine equations (1)–(3) to yield the governing equations for the pressure waves:

$$\frac{1}{\bar{\rho}\bar{c}^2}\left[\frac{\partial p'}{\partial t} - U_r \frac{\partial p'}{\partial y}\right] + \frac{\bar{C}_z}{\bar{\rho}\bar{c}^2}\left[\frac{\partial p'}{\partial z} + a_1 \frac{\partial p'}{\partial y}\right] + \frac{\partial q_z'}{\partial z} + \frac{\partial q_y'}{\partial y} = 0 \tag{4}$$

$$\frac{\partial q_z'}{\partial t} - U_r \frac{\partial q_z'}{\partial y} + \bar{C}_z\left[\frac{\partial q_z'}{\partial z} + a_1 \frac{\partial q_z'}{\partial y}\right] + \frac{1}{\bar{\rho}} \frac{\partial p'}{\partial z} = 0 \tag{5}$$

$$\frac{\partial q_y'}{\partial t} - U_r \frac{\partial q_y'}{\partial y} + \bar{C}_z\left[\frac{\partial q_y'}{\partial z} + a_1 \frac{\partial q_y'}{\partial y}\right] + \frac{1}{\bar{\rho}} \frac{\partial p'}{\partial y} = 0 \tag{6}$$

The Upstream Field

In the farfield ahead of the rotor the imposed shear wave distortion which satisfies relations (4) and (5) is given as

$$q_1' = \Delta q_0 \exp[i\omega\,(t + y/U_r - z a_1/U_r + \phi_0)] \tag{7}$$

where

$$a_1 = \tan \alpha_1$$

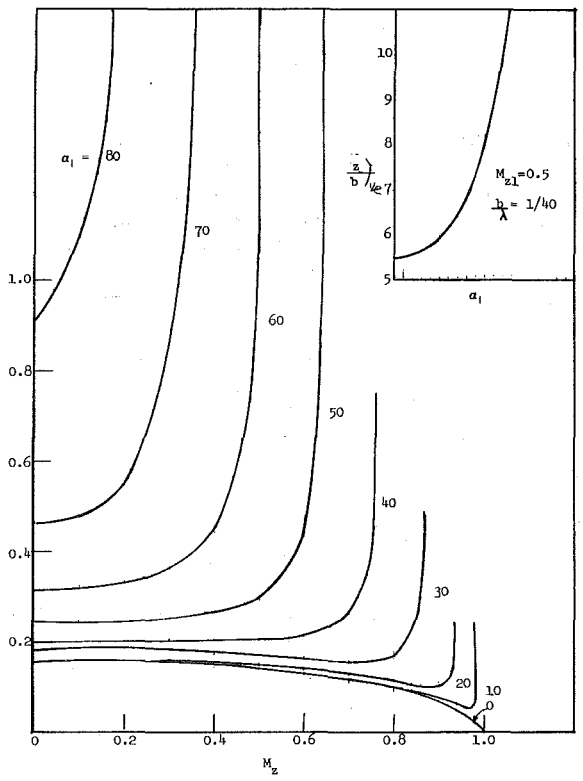

Fig. 2 Axial decay length versus axial Mach number at various swirl angles; $b/\lambda = 1/40$

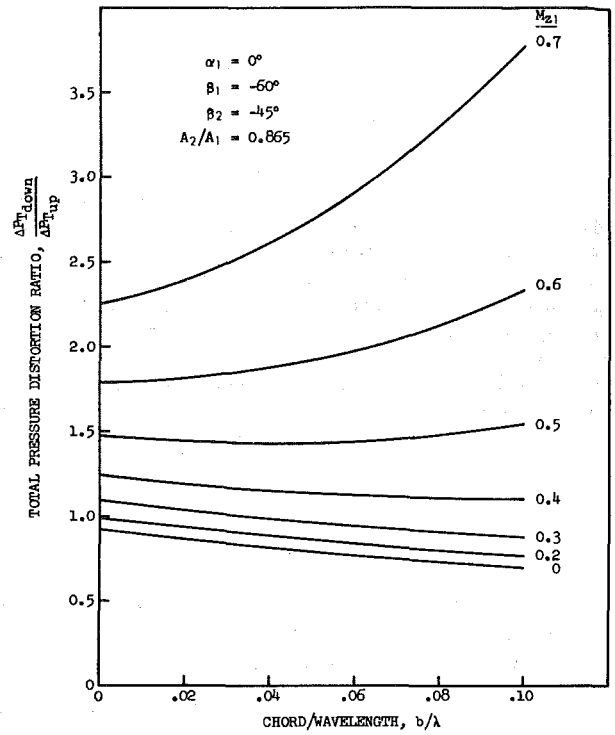

Fig. 3 Total pressure distortion transfer with b/λ at various axial Mach numbers. Operating line study with large axial gaps using SAD analysis.

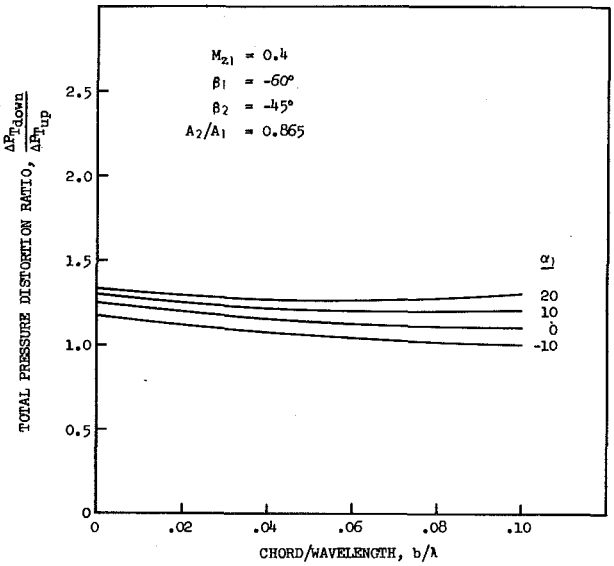

Fig. 4 Total pressure distortion transfer with b/λ at various inlet swirl angles. Operating line study with large axial gaps using SAD analysis.

and

$$\omega = \frac{2\pi U_r \cos \alpha_1}{\lambda} \tag{8}$$

The components in the axial and tangential direction (in either the absolute or relative coordinate system) are given by

$$q_{z1}' = \Delta C_{z1} = q_1' \cos \alpha_1$$

$$q_{y1}' = \Delta C_{\theta 1} = q_1' \sin \alpha_1 = a_1 \Delta C_{z1} \tag{9}$$

$$p_1' = 0$$

Near the rotor a pressure wave field is generated as a result of reflection of the imposed shear wave by the rotor; hence, at the rotor leading edge station 2

$$p_2' = p'$$

$$\rho_2' = p'/\bar{c}^2$$

$$q_{z2}' = \Delta C_{z1} + C_{z2}' \tag{10}$$

$$q_{y2}' = a_1 \Delta C_{z1} + C_{\theta 2}'$$

For all the waves existing both upstream and downstream of the cascade, the harmonic time dependence and phase velocities of the waves in the y-direction must be the same, since the peak and trough of one wave must be coincident with the peak and trough of the other wave, respectively, at the leading edge or trailing edge line of the cascade. In other words, the period and wave number in the cascade direction of the waves are uniquely determined by the incident wave. Hence the velocity and pressure description of the upstream pressure wave can be written as

$$C_z' = X(z) \exp[i\omega(t + y/U_r)]$$

$$C_\theta' = Y(z) \exp[i\omega(t + y/U_r)] \tag{11}$$

$$p' = P(z) \exp[i\omega(t + y/U_r)]$$

substituting into equations (4)–(6) yield the behavior of the fluid immediately ahead of the rotor as:

$$C_{z2}' = (A_{2R} + iA_{2I}) \exp[i\omega(t + y/U_r + d_1 r_1 z/U_R)] \exp[\omega f_1 r_1 z/U_r] \tag{12}$$

$$C_{\theta 2}' = [d_1 + if_1] C_{z2}' \tag{13}$$

$$p_2' = -\bar{\rho}\bar{C}_{z1}[e_1 + ia_1 f_1] C_{z2}' \tag{14}$$

$$r = \frac{1 - M_z^2 a^2}{1 - M_z^2}$$

$$d = \frac{a M_z^2}{1 - M_z^2 a^2} \tag{15}$$

$$e = \frac{1}{1 - M_z^2 a^2}$$

$$f = \frac{\sqrt{1 - M_z^2(1 + a^2)}}{1 - M_z^2 a^2}$$

The Downstream Field

Downstream of the cascade a shear wave and pressure wave will also exist. The perturbations due to the pressure wave can be obtained from (12)–(14) as:

$$C_{z3}' = (A_{3R} + iA_{3I}) \exp[i\omega(t + y/U_r + d_4 r_4 z/U_r)] \exp[-\omega f_4 r_4 z/U_r]$$

$$C_{\theta 3}' = (d_4 - if_4) C_{z3}' \tag{16}$$

$$p_3' = -\bar{\rho}_4 \bar{C}_{z4}(e_4 - ia_4 f_4) C_{z3}'$$

The complete velocity perturbations at the trailing edge plane are given by

$$q_{z3}' = C_{z3}' + \Delta C_{z4}$$

$$q_{y3}' = C_{\theta 3}' + \Delta C_{\theta 4} \tag{17}$$

At downstream infinity only the rotational shear wave will remain.

$$\Delta C_{z4} = (A_{4R} + iA_{4I}) \exp[i\omega(t + y/U_r - z a_4/U_r)]$$

$$\Delta C_{\theta 4} = a_4 \Delta C_{z4} \tag{18}$$

$$p_4' = 0$$

Flow Through the Cascade

The semiactuator disk approximation occurs in evaluating the field within the cascade. The assumption of infinitesimal blade spacing makes it possible to treat the flow in the cascade as one dimensional channel flow. The continuity, momentum and state

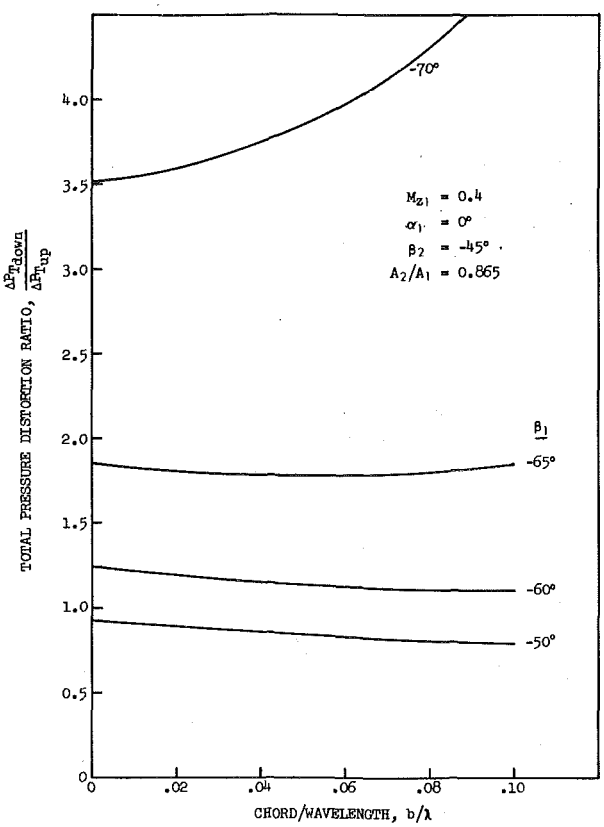

Fig. 5 Total pressure distortion transfer with b/λ at various inlet relative air angles. Operating line study with large axial gaps using SAD analysis.

equations for the perturbations become:

$$\frac{1}{\bar{\rho}_4}\left[\frac{\partial \rho'}{\partial t} + U\frac{\partial \rho'}{\partial \xi}\right] + \frac{\partial u}{\partial \xi} = 0$$

$$\frac{\partial u}{\partial t} + U\frac{\partial u}{\partial \xi} = -\frac{1}{\bar{\rho}_4}\frac{\partial p'}{\partial \xi}$$

$$\rho' = p'/\bar{c}_4^2$$

where U is the relative mean velocity in the cascade.

The mean quantities $\bar{\rho}_4$, and $\bar{c}_4^2$ are used since it is assumed that a mean flow singularity exists at the blade leading edge line.

The requirement of continuity of phase requires the circular frequency of the channel flow to be identical with the incident shear wave and requires the addition of the phase factor $\exp[i\omega y_0/U_r]$ to the final solution.

Then:

$$p' = P(\xi) \exp[i\omega(t + y_0/U_r)] \tag{19}$$

$$u' = \Xi(\xi) \exp[i\omega(t + y_0/U_r)] \tag{20}$$

The conservation equations become

$$\left[i\omega + U\frac{d}{d\xi}\right]\Xi = -\frac{1}{\bar{\rho}_4}\frac{dP}{d\xi}$$

$$\frac{1}{\bar{\rho}_4 \bar{c}_4^2}\left[i\omega + U\frac{d}{d\xi}\right]P = -\frac{d\Xi}{d\xi}$$

Solving the conservation equations, the pressure and velocity perturbations traveling within the cascade can be written as:

$$p' = \bar{\rho}_4 \bar{c}_4 \{D_u \exp[(iMk/(1 - M))(\xi/b)] - D_d \exp[(-iMk/(1 + M))(\xi/b)]\} \exp[i\omega(t + y_0/U_r)] \tag{21}$$

$$u' = \{D_u \exp[(iMk/(1 - M))(\xi/b)] + D_d \exp[(-iMk/(1 + M))(\xi/b)]\} \exp[i\omega(t + y_0/U_r)]$$

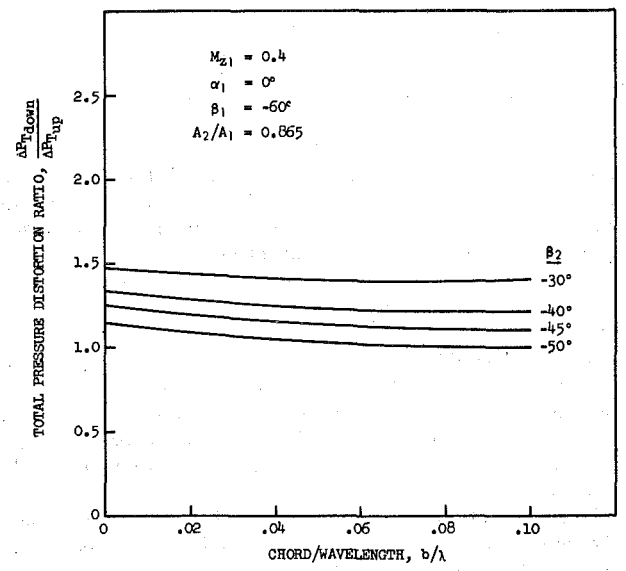

Fig. 6 Total pressure distortion transfer with b/λ at various blade exit angles. Operating line study with large axial gaps using SAD analysis.

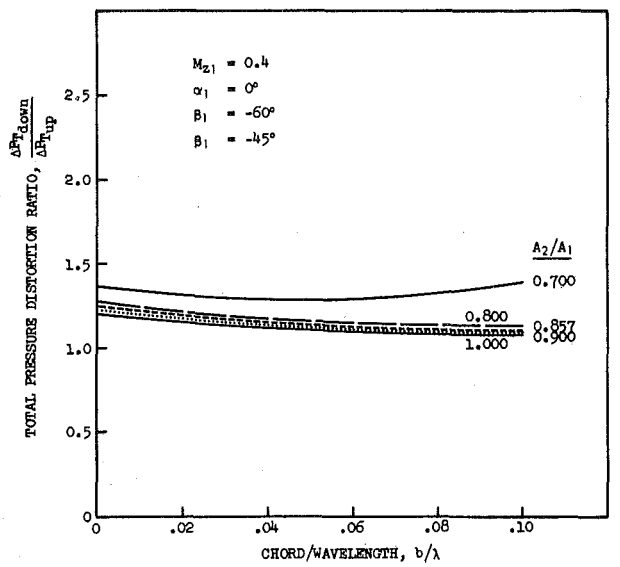

Fig. 7 Total pressure distortion transfer with b/λ at various contraction ratios, A_2/A_1. Operating line study with large axial gaps using SAD analysis.

where M is the relative Mach number, b is the blade chord and k is the reduced frequency:

$$k = \frac{\omega b}{U} \tag{22}$$

Communication Between Waves

Now that all of the fluctuating quantities in the flow fields are obtained, we shall consider the boundary conditions to be satisfied by them.

Leading Edge. The first requirement is that no mass will be lost in crossing the leading edge line. Considering the continuity equation in integral form and letting the control volume go to zero removes all reference to the unsteady processes occurring upstream or within the cascade. The conservation of mass flow then degenerates to the requirement that axial mass flux across the cascade inlet remains constant. After neglecting quadratic terms, the perturbation boundary condition becomes: (at $z = \xi = 0$ and $y = y_0$):

$$A_1[\,\bar{\rho}_1 q_{z2}' + \bar{C}_{z1}\rho_2'\,] = A_2[\,(\bar{\rho}_4 u_1' + U\rho_1' \cos\beta_2] \tag{23}$$

This type of argument cannot be applied to the momentum equation due to the leading edge singularity, thus it is necessary to introduce the concept of conservation of energy. Using the definition of linearized static enthalpy, the conservation of energy condition is written as:

$$p_2'/\bar{\rho}_1 + \bar{C}_{z1}q_{z2}' + C_{\theta 1}{}^R q_{y2}' = p_1'/\bar{\rho}_4 + Uu_1' \quad . \tag{24}$$

Trailing Edge. Equations (23) and (24) give the boundary equations required at the leading edge. Similar arguments can be applied to the trailing edge to give (at $\xi = b$; $z = b\cos\beta_2$; $y = y_0 + b\sin\beta_2$)

$$\bar{p}_4 q_{z3}' + \bar{C}_{z4}\rho_3' = (\bar{\rho}_4 u_t' + U\rho_t')\cos\beta_2 \tag{25}$$

and

$$\frac{p_3'}{\bar{\rho}_4} + \bar{C}_{z4}q_{z3}' + \bar{C}_{\theta 4}{}^R q_{y3}' = \frac{p_t'}{\bar{\rho}_4} + Uu_t' \tag{26}$$

If we assume that the rotor is heavily bladed, the relative exit air angle of the fluid leaving the rotor will coincide with the geometric exit blade angle irrespective of the relative incidence angle. This assumption, known as the Kutta-Joukowski condition, is commonly used in thin airfoil theory and has been proven to be a necessary condition to eliminate flow singularities from the airfoil trailing edge, insuring a unique solution to the potential flow problem. Physically it is interpreted as a limiting effect of viscosity.

The Kutta-Joukowski condition can be expressed as

$$\begin{aligned} \bar{C}_{z4} + q_{z3}' &= (U + u_t')\cos\beta_2 \\ \bar{C}_{\theta 4}{}^R + q_{y3}' &= (U + u_t')\sin\beta_2 \end{aligned} \tag{27}$$

So that the mean flow:

$$C_{z4} = U\cos\beta_2 \tag{28}$$

$$C_{\theta 4}{}^R = U\sin\beta_2 = \bar{C}_{z4}b_3 \tag{29}$$

where $b_3 = \tan\beta_2$ and for the perturbations:

$$\begin{aligned} q_{z3}' &= u_t'\cos\beta_2 \\ q_{y3}' &= u_t\sin\beta_2 = b_3 q_{z3}' \end{aligned} \tag{30}$$

Substituting (28) and (30) into either equation (25) or (26) gives

$$p_3' = p_t' \tag{31}$$

Either equation (30) or (31) can be used as the coupling boundary condition at the trailing edge line of the cascade.

Final System of Equations

For a given incident shear wave, relations (23)–(26) and (30) give five equations for the five unknown wave forms.

These relations can be expressed in the matrix form

$$\tilde{C}_{ij}\tilde{X}_j = \tilde{B}_i \tag{32}$$

The unknown amplitude column vector $\tilde{X}$ is given by

$$\tilde{X} = \begin{bmatrix} \frac{X_{2I}}{\epsilon_1} \\ \frac{X_{2R}}{\epsilon_1} \\ \frac{X_{3I}}{\epsilon_1} \\ \frac{X_{3R}}{\epsilon_1} \\ \frac{X_{4I}}{\epsilon_1} \\ \frac{X_{4R}}{\epsilon_1} \end{bmatrix} = \begin{bmatrix} \frac{\epsilon_2}{\epsilon_1}\sin\phi_2 \\ \frac{\epsilon_2}{\epsilon_1}\cos\phi_2 \\ \frac{\epsilon_3}{\epsilon_1}\exp[-kf_4r_4/(b_3-a_4)]\sin[\phi_3 + k(d_4r_4 + a_4)/(b_3-a_4)] \\ \frac{\epsilon_3}{\epsilon_1}\exp[-kf_4r_4/(b_3-a_4)]\cos[\phi_3 + k(d_4r_4 + a_4)/(b_3-a_4)] \\ \frac{\epsilon_4}{\epsilon_1}\sin\phi_4 \\ \frac{\epsilon_4}{\epsilon_1}\cos\phi_4 \end{bmatrix} \tag{33}$$

The elements of the coefficient matrix $\tilde{C}_{ij}$ and the column vector $\tilde{B}_j$ are defined in Appendix A.

Limiting Cases

The correctness of the matrix form (32) can be checked by considering two degenerate solutions: (1) incompressible actuator disk and (2) isolated stator row where previously derived solutions exist. In addition, reduced forms for the incompressible semiactuator disk and the compressible actuator disk can be formulated.

To obtain the incompressible actuator disk formulation one can simultaneously let the reduced frequency and Mach number go to zero in matrix (32) to give:

$$\begin{bmatrix} \bar{C}_{z4}/\bar{C}_{z1} & 0 & -1 & 0 & -1 & 0 \\ 0 & \bar{C}_{z4}/\bar{C}_{z1} & 0 & -1 & 0 & -1 \\ 0 & 0 & 1 & -b_3 & 0 & -(b_3-a_4) \\ 0 & 0 & b_3 & 1 & (b_3-a_4) & 0 \\ 0 & -(b_3-a_4) & 0 & -(b_3-a_4) & 1+b_3a_4 & 0 \\ b_3-a_4 & 0 & b_3-a_4 & 0 & 0 & 1+b_3a_4 \end{bmatrix}$$

$$\begin{bmatrix} \epsilon_2/\epsilon_1 \sin\phi_2 \\ \epsilon_2/\epsilon_1 \cos\phi_2 \\ \epsilon_3/\epsilon_1 \sin\phi_3 \\ \epsilon_3/\epsilon_1 \cos\phi_3 \\ \epsilon_4/\epsilon_1 \sin\phi_4 \\ \epsilon_4/\epsilon_1 \cos\phi_4 \end{bmatrix} = \begin{bmatrix} 0 \\ -\bar{C}_{z4}/\bar{C}_{z1} \\ 0 \\ 0 \\ 0 \\ 1+a_1^2+a_1(b_3-a_4) \end{bmatrix} \tag{34}$$

This form is seen to be identical to equation (18) of Ehrich's paper [7] including the effect of velocity across the stage.

The case of an isolated stator row can be obtained by setting the rotor speed to zero:

$$U_r = b_3 - a_4 = (\bar{C}_{z1}/\bar{C}_{z4})\,(b_2 - a_1) = 0$$

Equations (22) and (9) then give

$$k = 0$$

so the matrix equation becomes:

$$\begin{bmatrix} C_{11} & C_{12} & C_{13} & C_{14} & -1 & 0 \\ -C_{12} & C_{11} & -C_{14} & C_{13} & 0 & -1 \\ 0 & 0 & C_{33} & C_{34} & 0 & 0 \\ 0 & 0 & -C_{34} & C_{33} & 0 & 0 \\ 0 & 0 & 0 & 0 & C_{55} & 0 \\ 0 & 0 & 0 & 0 & 0 & C_{55} \end{bmatrix} \begin{bmatrix} X_{2I} \\ X_{2R} \\ X_{3I} \\ X_{3R} \\ X_{4I} \\ X_{4R} \end{bmatrix} = \begin{bmatrix} B_1 \\ B_2 \\ 0 \\ 0 \\ B_5 \\ B_6 \end{bmatrix} \tag{35}$$

The solution to this system is simply

$$\left(\frac{\epsilon_4}{\epsilon_1}\right)_{\text{stator}} = \frac{\bar{C}_{z1}}{\bar{C}_{z4}} \frac{(1+a_1^2)}{(1+a_4^2)} \tag{36}$$

$$\phi_4 = \phi_1$$

which is the relation for the axial velocity distortion. This relation is exactly that found by Ehrich [7] and is seen to be void of any compressibility or unsteady effects. Substituting into the expression for the total pressure distortion produces the expected result that neither the total pressure amplitude or wave shape is changed in crossing a stator.

Field Equations

The solution of equation (32) produces the solution vector given by (33) in terms of the velocity ratios ϵ_2/ϵ_1, ϵ_3/ϵ_1, ϵ_4/ϵ_1 and phase: ϕ_2, ϕ_3, and ϕ_4. This may be related to the local static pressure, axial velocity and swirl velocity distortion on either side of the rotor by using equations (12)–(18).

Upstream of the Rotor. The axial velocity distortion ahead of the rotor is determined by the sum of the imposed velocity distortion and the velocity field reflected from the rotor

$$\Delta C_{zu} = \Delta C_{z1} + C_{z2}$$

From equations (9) and (12) we obtain

$$\Delta C_{zu} = \epsilon_1 \exp\{i[k(\theta - a_1 z)/(b_3 - a_4) + \phi_1]\} + \epsilon_2 \exp[kf_1 r_1 z/(b_3 - a_4)] \cdot \exp\{i[k(\theta + d_1 r_1 z/(b_3 - a_4) + \phi_2]\} \tag{37}$$

The swirl velocity distortion is similarly stated by

$$\Delta C_{\theta u} = \Delta C_{\theta 1} + C_{\theta 2}'$$

where the relationships in fields 1 and 2 are given by equations (9) and (13), respectively, i.e.,

$$\Delta C_{\theta u} = \epsilon_1 a_1 \exp\{i[k(\theta - a_1 z)/(b_3 - a_4) + \phi_2]\} + \epsilon_2 (d_1 + if_1) \exp[kf_1 r_1 z/(b_3 - a_4)] \exp\{i[k(\theta + d_1 r_1 z/(b_3 - a_4) + \phi_2]\} \tag{38}$$

The static pressure distortion is obtained from equation (14) as:

$$\Delta p_u = p_2' = -\bar{\rho}_1 \bar{C}_{z1} \epsilon_1 (e_1 + i a_1 f_1) \exp[k_1 f_1 z r_1/(b_3 - a_4)] \exp\{i[k(\theta + r_1 d_1 z)/(b_3 - a_4) + \phi_2]\} \tag{39}$$

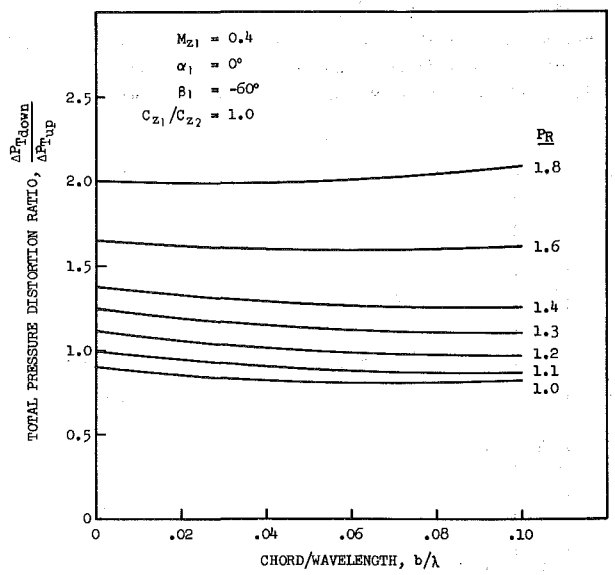

Fig. 8 Total pressure distortion transfer with b/λ at various pressure ratios. Design point study with large axial gaps using SAD analysis.

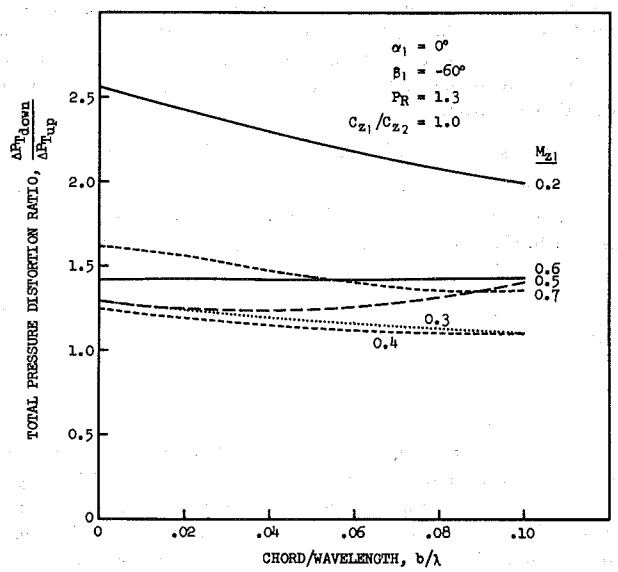

Fig. 9 Total pressure distortion transfer with b/λ at various axial Mach numbers. Design point study with large axial gaps using SAD analysis.

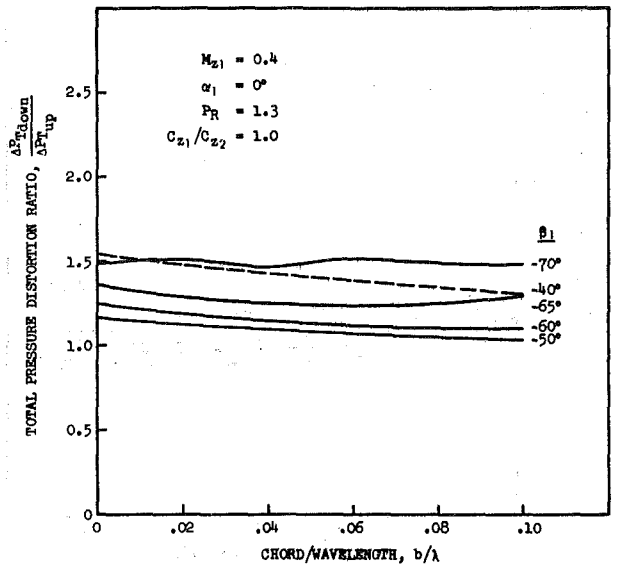

Fig. 10 Total pressure distortion transfer with b/λ at various inlet relative air angles. Design point study with large axial gaps using SAD analysis.

Downstream of the Rotor. Behind the rotor the field composition is similar to upstream. Equations (15) to (17) and (33) give

$$\Delta C_{zD} = \epsilon_4 \exp\{i[k(\theta - a_4 z)/(b_3 - a_4) + \phi_4]\} + \epsilon_3 \exp[-kr_4 f_4 z/(b_3 - a_4)]. \quad (40)$$

$$\exp\{i[k(\theta + d_4 r_4 z)/(b_3 - a_4) + \phi_3]\} \quad (41)$$

$$\Delta C_{\theta D} = \epsilon_4 a_4 \exp\{i[k(\theta - a_4 z)/(b_3 - a_4) + \phi_4]\} + \epsilon_3 (d_4 - if_4) \exp[-kf_4 r_4 z/(b_3 - a_4)]. \quad (42)$$

$$\exp\{i[k(\theta + d_4 r_4 z)/(b_3 - a_4) + \phi_3]\}$$

$$\Delta p_D = p_3' = -\bar{\rho}_4 \bar{C}_{z4} \epsilon_4 (e_4 - i a_4 f_4) \exp[-kf_4 r_4 z/(b_3 - a_4)].$$

$$\exp\{i[k(\theta + d_4 r_4 z)/(b_3 - a_4) + \phi_3]\}$$

Both the upstream and downstream fields contain exponential terms which create a static pressure distortion near the rotor and wash out the velocity distortion. In general one would like to place instrumentation far enough away from the rotor to avoid these induced fields. Equation (12) shows that the amplitude of the induced distortion has decayed to $1/e$ of its initial level when

$$\frac{\omega z}{U_r} \frac{\sqrt{1 - M_z^2(1 + a_1^2)}}{1 - M_z^2} = 1$$

or

$$\frac{z}{\lambda} = \frac{1 - M_z^2}{2\pi\sqrt{1 - M_z^2(1 + a_1^2)}}. \quad (43)$$

This relation is plotted in Fig. 2. Note that the dependence vanishes when the absolute Mach number exceeds 1 so that the term under the radial changes sign.

Total Pressure Distortion

Defining the distortion amplitude as the difference between the maximum (or minimum) level and the average, a relationship was derived between total pressure and the local static pressure and velocity. Using the isentropic relation for the total to static pressure ratio and the definition for the speed of sound, the total pressure perturbations can be expressed in terms of static values as:

$$\Delta P_T/P_T = \frac{p'/\bar{p} + \gamma M_z(1 + a^2)(C_z'/\bar{c} + aC_\theta'/\bar{c})}{1 + [(\gamma - 1)/2]M_z^2(1 + a^2)} \quad (44)$$

Recalling that the static pressure and swirl velocity distortion decay exponentially from the blade row we see that the total pressure upstream and down can simply be obtained from

$$\left(\frac{\Delta P_T}{P_T}\right)_{up} = [\gamma M_{z1}(1 + a_1^2)(\Delta C_{z1}/\bar{c}_1)]/[1 + ((\gamma - 1)/2)M_{z1}^2(1 + a_1^2)]$$

$$\left(\frac{\Delta P_T}{P_T}\right)_{down} = [\gamma M_{z4}(1 + a_4^2)(\Delta C_{z4}/c_4)]/[1 + ((\gamma - 1)/2)M_{z4}^2(1 + a_4^2)] \quad (45)$$

These relations can be verified by direct substitution to give

$$\Delta P_{T4}/\Delta P_{T1} = (P_{T4}/P_{T1})^{(1/\gamma)}(1 + a_4^2)/(1 + a_1^2)[(\epsilon_4/\epsilon_1)/(\bar{C}_{z1}/\bar{C}_{z4})] \quad (46)$$

Square Wave and Arbitrary Distortion Waveform

The analysis derived in this paper has assumed the upstream distortion is sinusoidal, given by the relation

$$\Delta q = \Delta q_0 \exp[i(2\pi\theta/\lambda + \phi_0)]$$

This restriction may easily be relieved to any arbitrary wave shape by the use of Fourier series. A waveform Δq can then be represented by

$$\Delta q = \sum_{n=-\infty}^{\infty} C_n \exp[i(2\pi n\theta/\lambda - \phi_n)] = \sum_{n=1}^{\infty} C_n \cos(2\pi n\theta/\lambda - \phi_n) \quad (47)$$

where

$$C_n = \sqrt{A_n^2 + B_n^2} \quad (48)$$

$$\phi_n = \tan^{-1}(B_n/A_n)$$

$$A_n = 2/\lambda \int_0^\lambda \Delta q \cos(2\pi n\theta/\lambda) d\theta$$

$$B_n = 2/\lambda \int_0^\lambda \Delta q \sin(2\pi n\theta/\lambda) d\theta$$

The coefficient A_0 is not used because the mean value of the distortion perturbation is by definition zero. In particular a one per rev square wave with a defect of extent θ_{ext} centered at 180 deg gives

$$C_n = 2 \sin(\theta_{ext} n/2)/\pi n$$

$$\phi_n = \begin{cases} \pi & ; \quad n \text{ odd} \\ 0 & ; \quad n \text{ even} \end{cases} \quad (49)$$

Relation of Compressor Design Parameters to the Computer Input

The semiactuator disk analysis was developed to study realistic systems which have a total pressure change and turning across the stage. This section presents the results of a parametric study showing the influence of stage design parameters on the transmission of an inlet distortion through a rotor under different operating conditions and for a number of rotors at their design points.

The coefficient matrix $\bar{C}_{ij}$ and the column matrix $\bar{B}_i$ are seen to be functions of k, M, M_{z1}, M_{z4}, a_1, b_2, b_3, a_4, $\bar{\rho}/\rho_4$ and $\bar{C}_{z1}/\bar{C}_{z4}$. In this section we will define these quantities in terms of normally specified compressor design parameters and show their interdependence.

The density ratio $\bar{\rho}_1/\bar{\rho}_4$ and the velocity ratio $\bar{C}_{z1}/\bar{C}_{z4}$ are related by continuity

$$\bar{\rho}_1/\bar{\rho}_4 = 1/(\bar{C}_{z1} AR/\bar{C}_{z4}) \quad (50)$$

where

$$AR = A_1/A_2 \quad (51)$$

is the stream tube contraction across the blade row.

One would normally specify either AR or $\bar{C}_{z1}/\bar{C}_{z4}$ depending on the application and calculate the other from (50) using the density ratio from the isentropic relation

$$\frac{\bar{\rho}_1}{\bar{\rho}_2} = \frac{\bar{\rho}_{T1}}{\bar{\rho}_{T2}} \left[\frac{1 + \frac{\gamma - 1}{2} M_{z4}^2 (1 + a_4^2)}{1 + \frac{\gamma - 1}{2} M_{z1}^2 (1 + a_1^2)} \right]^{(1/(\gamma-1))} \tag{52}$$

The upstream Mach number M_{z1} is a known input parameter from the weight flow. The downstream axial Mach number, M_{z4}, is obtained in terms of the remaining parameters from:

$$M_{z4} = M_{z1} \Big/ \sqrt{(\bar{C}_{z1}/\bar{C}_{z4})^2 (T_{T4}/T_{T1}) [1 + ((\gamma - 1)/2) M_{z1}^2 (a_1^2 - a_4^2)]} \tag{53}$$

Recalling that all thermodynamic changes are assumed to take place at the leading edge, the relative Mach number is given by:

$$M = M_{z4}/\cos \beta_2 = M_{z4} \sqrt{1 + b_3^2} \tag{54}$$

Furthermore, equation (22) gives the reduced frequency as

$$k = 2\pi b U_r \cos \alpha_1 / \lambda U = [2\pi (b/\lambda)(b_3 - a_4)] / \sqrt{(1 + b_3^2)(1 + a_1^2)}$$

Operating Line Study

In the case of an existing fan operating at off design, one normally has readily available information on the airflow, rotor speed, flowpath inlet swirl and blade angles. From these items the inlet axial Mach number M_{z1} is obtained from the flow; the inlet absolute swirl angle α_1 is obtained from the OGV setting. The inlet relative air angle β_1 is obtained from the flow and rotor speed; the area ratio AR is known from the flowpath and the exit relative air angle β_2 is found from the blade geometry. With this set of input variables the axial velocity ratio across the rotor is obtained by iterating equations (50), (52), and (53). The prescribed input is then obtained from

$$\begin{aligned} a_1 &= \tan \alpha_1 \\ b_2 &= \tan \beta_1 \\ b_3 &= \tan \beta_2 \\ a_4 &= b_3 - (b_2 - a_1)\, \bar{C}_{z1}/\bar{C}_{z4} \end{aligned} \tag{55}$$

The influence of inflow Mach number holding the inlet swirl, relative air angles and contraction ratio constant is shown in Fig. 3. A significant conclusion is that the effect of increasing chord or distortion zone has an attenuating effect at low Mach number but amplifies the distortion at high Mach number. This has bearing on the relative importance of low speed compressor testing. Fig. 4 shows the influence of preswirl on the distortion transfer. Inducing a swirl in the opposite direction from rotor rotation is found to have an attenuating effect since the inlet relative air angle is held fixed. This case also corresponds to reducing the rotor speed with a fixed flow. Decreasing the relative inlet air angle (or increasing flow coefficient) can significantly reduce the distortion transfer through the stage as seen in Fig. 5. At high angle increasing b/λ will increase the distortion after the rotor. At nominal and low values, the reverse is true.

In the case of a fixed inlet angle, changing the rotor blade setting to produce a higher discharge angle will attenuate the distortion as shown in Fig. 6. The influence of contraction ratio is shown in Fig. 7.

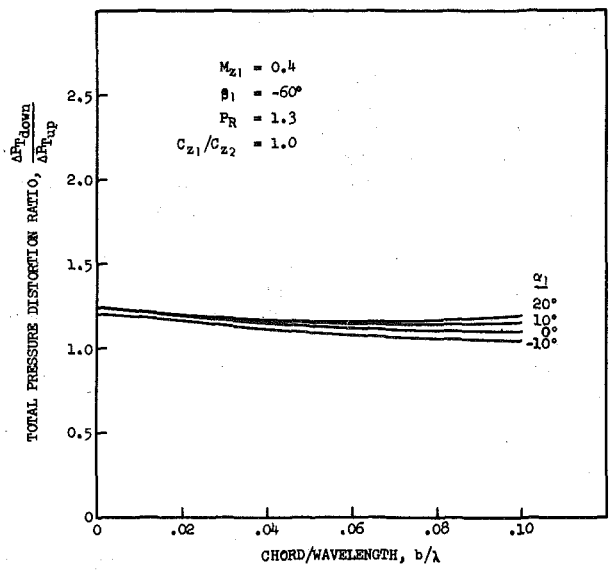

Fig. 11 Total pressure distortion transfer with b/λ at various inlet angles. Design point study with large axial gaps using SAD analysis.

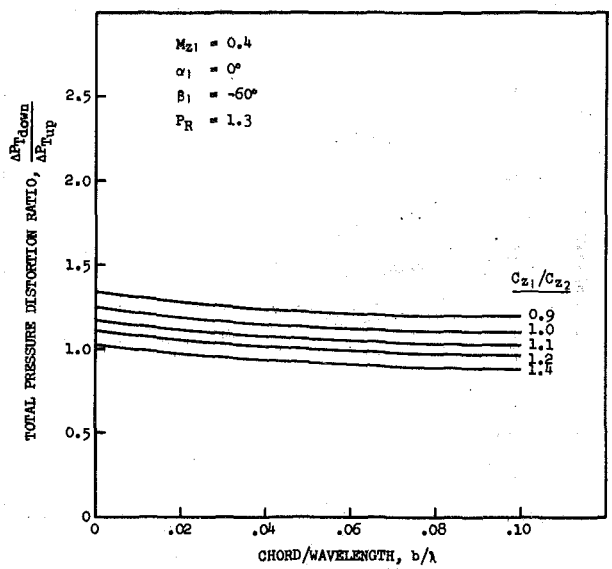

Fig. 12 Total pressure distortion transfer with b/λ at various axial velocity ratios. Design point study with large axial gaps using SAD analysis.

Design Point Study

In the case where only fan design concepts are being analyzed one normally defines each fan by its flow, pressure ratio, tip speed, axial velocity ratio and inlet swirl angle.

Again flow, tip speed and inlet swirl give M_{z1}, a_1, and b_2 directly. Total pressure ratio is related to total temperature ratio in this "no loss" rotor by the isentropic expression

$$T_{T4}/T_{T1} = (P_{T4}/P_{T1})^{((\gamma-1)/\gamma)} \tag{56}$$

The steady state energy is given by

$$c_p T_{T1} [(T_{T4}/T_{T1}) - 1] = U_r (\bar{C}_{\theta 4} - \bar{C}_{\theta 1}) = U_r \bar{C}_{z1} (a_4 \bar{C}_{z4}/\bar{C}_{z1} - a_1)$$

which can be rearranged to give a_4 as

$$a_4 = \left\{ a_1 + \frac{[(T_{T4}/T_{T1}) - 1][1 + ((\gamma - 1)/2) M_{z1}^2 (1 + a_1^2)]}{(\gamma - 1) M_{z1}^2 (b_2 - a_1)} \right\} \bar{C}_{z1}/\bar{C}_{z4} \tag{57}$$

and the tip speed relation gives

$$b_3 = a_4 + (b_2 - a_1)\, \bar{C}_{z1}/\bar{C}_{z4}$$

With a_4 determined, M_{z4} can be obtained from equation (53) and the area ratio is immediately found from (50) and (52).

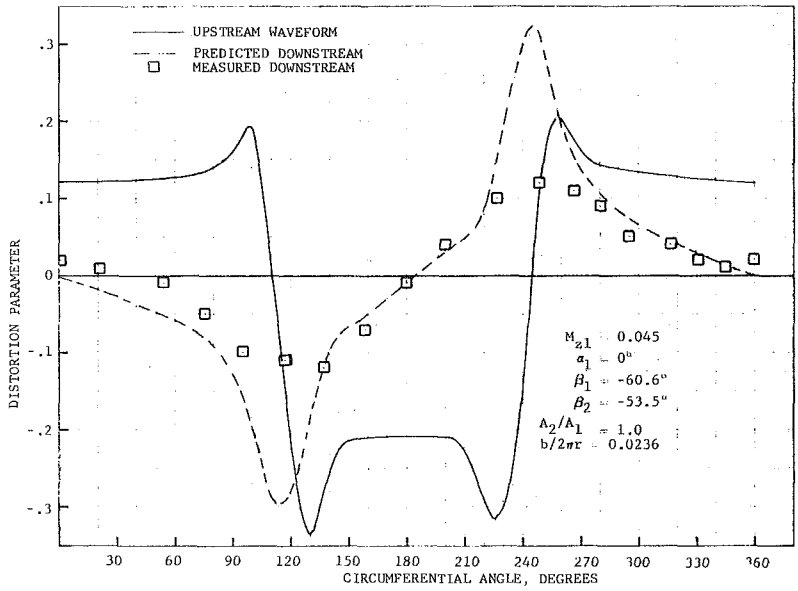

Fig. 13 Comparison between theory and the experiments of Seidel; rotor alone using SAD analysis.

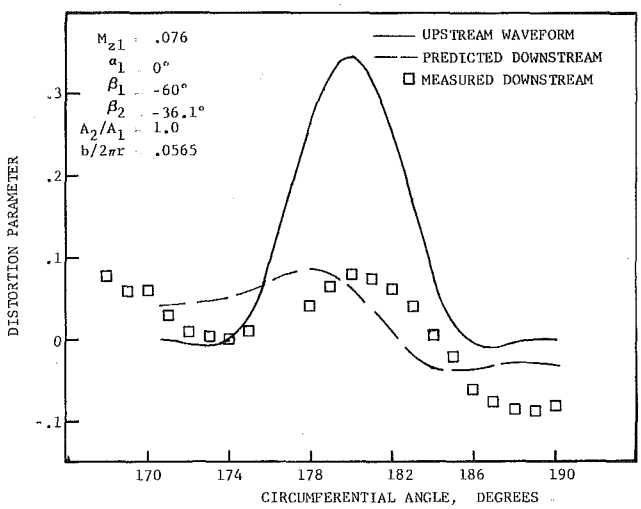

Fig. 14 Comparison between theory and the experiments of Ashby; rotor alone, $\beta_1 = -60$ deg using SAD analysis.

Stage pressure ratio is seen to have a strong amplifying effect on the distortion in Fig. 8. This is consistent with the general experimental observation that a highly loaded fan is more sensitive to inlet distortions than a lightly loaded fan. At moderate pressure ratios, increasing rotor chord has an attenuating influence.

The effect of axial Mach number and flow with a fixed pressure ratio and flow coefficient is shown in Fig. 9. The low Mach numbers are seen to have high transfer coefficients because of the large amount of turning required to produce 1.3 pressure ratio at low flows. Increasing the inlet air angle with a fixed flow and pressure ratio results in an amplifying effect in Fig. 10. At high angles, the solution exhibits a periodic variation with b/λ.

It is seen from Fig. 11 that the inclusion of a swirl counter to rotor rotation gives a lower total pressure distortion transfer and causes blade chord to have a stronger attenuating influence. The axial velocity distortion on the other hand, increased with counter swirl. This is a result of a larger increase in the term $(1 + a_4^2)/(1 + a_1^2)$ in equation (46) than a decrease in ϵ_4/ϵ_1 when swirl angle is increased. Ehrich [7] reports an attenuation of axial velocity distortion with inducing a swirl in the direction of rotor which was also experienced in the present analysis.

Designing a fan with a lower axial velocity after the stage is predicted to improve the distortion transfer in Fig. 12. A general observation can be made from Figs. 3–12. In the domain of typical compressor design and operation, the distortion transfer is relatively insensitive to changes in rotor chord or distortion wavelength. This conclusion justifies the use of steady flow analysis for the inlet distortion problem for a low speed machine.

Comparison Between Theory and Experiment

A number of experiments have been conducted to study the transfer characteristics of a rotor. Seidel [4] measured the response of a low speed isolated rotor to a 120 deg square wave. The prediction method is seen to reproduce Seidel's [4] measured data in Fig. 13 except at the maximum peak deviations occurring at the edge of input wave. Katz [5] has shown that such peaks are rounded off if viscous losses within the cascade are taken into account.

Ashby [11] inserted a ¼-in. rod ahead of an isolated low speed rotor. A comparison with his data is given in Fig. 14. Excellent agreement is obtained particularly where the measure reflex in the wake is reproduced by the theory.

Conclusions

Semiactuator disk theory is used to study the unsteady response of a rotor to stationary circumferential inlet distortion. The analytical results show:

1 In the range of typical compressor design and operation, the SAD method shows the distortion transfer to be relatively insensitive to rotor chord or distortion wavelengths.

2 With a fixed design, increasing blade chord will attenuate the distortion at low Mach number but can amplify at high Mach number.

3 For a fixed design at different operating lines, lower distortion transfer occurred with: *(a)* Preswirl in the direction of rotor rotation; *(b)* decreasing the relative inlet air angle; *(c)* increased exit relative air angle.

4 For a number of design fans, reduced distortion transfer occurred with: *(a)* Lower design pressure ratio; *(b)* lower inlet relative air angle; *(c)* preswirl in the direction of rotor rotation; *(d)* increased axial velocity ratio.

5 Excellent agreement between theory and experiment was obtained.

Acknowledgment

The authors would like to thank Mr. Phil Gliebe of the General Electric Company for his many helpful suggestions and comments during the course of this work.

References

1 Langston, C. B., Distortion Tolerance by Design Instead of by Accident," ASME Paper No. 69-GT-19.

2 Cotter, H. N., "Integration of Inlet and Engine—An Engine Man's Point of View," SAE Paper 680286, 1968.

3 Reid, C. L., "The Response of Axial Flow Compressors to Intake Flow Distortion," ASME Paper No. 69-GE-29.

4 Seidel, B. S., "Asymmetric Inlet Flow in Axial Turbomachines," TRANS. ASME, Series A, Vol. 86, Jan. 1964, p. 18.

5 Katz, R., "Performance of Axial Compression With Asymmetric Inlet Flows," Cal. Inst. of Tech. Report AFOSR TR-58-89, 1958.

6 Gliebe, P. R., "Compressible Flow Actuator Disc Analysis for Cascades With Inlet Distortion," unpublished.

7 Ehrich, F. F., "Circumferential Inlet Distortions in Axial Flow Turbomachinery," JAS, Vol. 24, No. 6, June 1957, pp. 413–417.

8 Tanida, Y., and Okazaki, T., "Stall Flutter in Cascade (3rd Report: Arbitrary Mode Vibration of Cascade Blades as Treated by Semi-Actuator Disc Method)," *JSME Bulletin,* Vol. 11, No. 48, Dec. 1968.

9 Kaji, S., and Okazaki, T., "Propagation of Sound Waves Through a Blade Row; I: Analysis Based on the Semi-Actuator Disc Theory," *J. Sound and Vibration,* Vol. 11, No. 3, 1970, pp. 339–353.

10 Alford, J. S., "Design Criteria and Configuration for Long Life Aircraft Gas Turbines," Appendix C: "Oscillatory Flows in Periodic Structures," SAE Paper 670344, 1967.

11 Ashby, G. C., "Investigation of the Effect of Velocity Diagram on Inlet Total Pressure Distortion Through a Single Stage Subsonic Flow Compressors," NACA RML57A03, 1957.

APPENDIX A

Definition of Matrix Elements

The elements of the coefficient matrix $\tilde{C}_{ij}$ are:

$$\tilde{C}_{11} = \tilde{C}_{22} = (\bar{C}_{z4}/\bar{C}_{z1})\ (1 - M_{z1}^2 e_1)$$

$$\tilde{C}_{12} = -\tilde{C}_{21} = -(\bar{C}_{z4}/\bar{C}_{z1}) M_{z1}^2 a_1 f_1$$

$$\tilde{C}_{13} = \tilde{C}_{24} = -g + M_{z4}^2 (m e_4 + n a_4 f_4)$$

$$\tilde{C}_{14} = -\tilde{C}_{23} = -h + M_{z4}^2 (n e_4 - m a_4 f_4) \qquad \text{(A1)}$$

$$\tilde{C}_{15} = \tilde{C}_{26} = -g$$

$$\tilde{C}_{16} = -\tilde{C}_{25} = -h$$

$$\tilde{C}_{31} = \tilde{C}_{32} = \tilde{C}_{35} = \tilde{C}_{41} = \tilde{C}_{42} = \tilde{C}_{46} = 0$$

$$\tilde{C}_{33} = \tilde{C}_{44} = f_4$$

$$\tilde{C}_{34} = -\tilde{C}_{43} = d_4 - b_3$$

$$\tilde{C}_{36} = -\tilde{C}_{45} = a_4 - b_3 = -U_r/\bar{C}_{z4}$$

$$\tilde{C}_{51} = \tilde{C}_{62} = -(\bar{C}_{z1}/\bar{C}_{z4})(1 - e_1 + b_2 d_1) = (b_3 - a_4) d_1$$

$$\tilde{C}_{52} = -\tilde{C}_{61} = (\bar{C}_{z1}/\bar{C}_{z4}) f_1 (a_1 - b_2) = f_1 (a_4 - b_3)$$

$$\tilde{C}_{53} = \tilde{C}_{64} = (1 + b_3^2) m - h a_4 f_4 - g e_4 + b_3 (d_4 - b_3) \qquad \text{(A1)}$$

$$\tilde{C}_{54} = -\tilde{C}_{63} = (1 + b_3^2) n - h e_4 + g a_4 f_4 - b_3 f_4$$

$$\tilde{C}_{55} = \tilde{C}_{66} = (1 + b_3^2)(m + b_3 (a_4 - b_3)$$

$$\tilde{C}_{56} = -\tilde{C}_{65} = (1 + b_3^2) n$$

where

$$g = \cos\left(\frac{kM}{1 - M^2}\right) \cos\left(\frac{kM^2}{1 - M^2}\right) - M \sin\left(\frac{kM}{1 - M^2}\right) \sin\left(\frac{kM^2}{1 - M^2}\right)$$

$$h = -\cos\left(\frac{kM}{1 - M^2}\right) \sin\left(\frac{kM^2}{1 - M^2}\right) - M \sin\left(\frac{kM}{1 - M^2}\right) \cos\left(\frac{kM^2}{1 - M^2}\right)$$

$$m = -\frac{1}{M} \sin\left(\frac{kM}{1 - M^2}\right) \sin\left(\frac{kM^2}{1 - M^2}\right) + \cos\left(\frac{kM}{1 - M^2}\right) \cos\left(\frac{kM^2}{1 - M^2}\right)$$

$$n = -\frac{1}{M} \sin\left(\frac{kM}{1 - M^2}\right) \cos\left(\frac{kM^2}{1 - M^2}\right) - \cos\left(\frac{kM}{1 - M^2}\right) \sin\left(\frac{kM^2}{1 - M^2}\right) \qquad \text{(A2)}$$

The column vector $\tilde{B}i$ is given by

$$\tilde{B} = \begin{bmatrix} -\bar{C}_{z4}/\bar{C}_{z1} \sin\phi_1 \\ -\bar{C}_{z4}/\bar{C}_{z1} \cos\phi_1 \\ 0 \\ 0 \\ [(\bar{C}_{z1}/\bar{C}_{z4})\ (1 + a_1^2) + a_1 (b_3 - a_4)] \sin\phi_1 \\ [(\bar{C}_{z1}/\bar{C}_{z4})\ (1 + a_1^2) + a_1 (b_3 - a_4)\ ] \cos\phi_1 \end{bmatrix} \qquad \text{(A3)}$$

The vector $\tilde{X}$ is solved using the matrix inverse.